



UNIVERSITY OF MICHIGAN 

NERS/BIOE 481

Lecture 05
Radiographic Image Formation

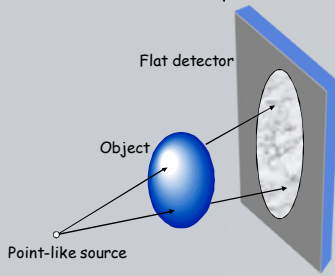
Michael Flynn, Adjunct Prof
Nuclear Engr & Rad. Science
mikef@umich.edu
mikef@rad.hfh.edu



RADIOLOGY RESEARCH

IV.A.1 - Transmission geometry

The radiographic image formation process projects the properties of the object along straight lines from a point-like source to various positions on a detector surface.



- The recorded signal reflects material properties encountered along each ray path.
- Distortion of the object can occur if the detector surface is oblique

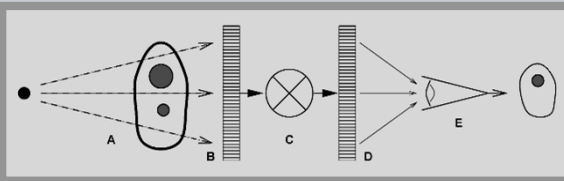
The radiographic projection is a 'perspective transmissive projection' from the point of view of the source. Object features close to the source are magnified as are visual objects close to the viewer eye.

NERS/BIOE 481 - 2019 4

IV - General Model - xray imaging

Xrays are used to examine the interior content of objects by recording and displaying transmitted radiation from a point source.

DETECTION
DISPLAY

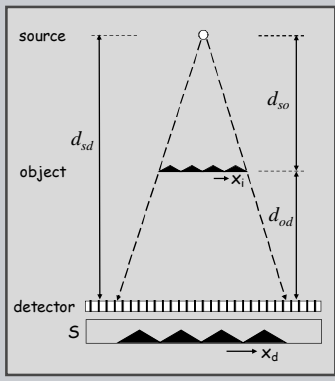


- (A) Subject contrast from radiation transmission is
- (B) recorded by the detector and
- (C) transformed to display values that are
- (D) sent to a display device for
- (E) presentation to the human visual system.

NERS/BIOE 481 - 2019 2

IV.A.2 - Magnification, M

The diverging path of the x-rays caused the recorded signal, S, in relation to detector position, x_d , to be magnified relative to the object size, x_o .



$$M = \frac{d_{sd}}{d_{so}}$$

$$= (d_{so} + d_{od}) / d_{so}$$

$$= 1 + d_{od} / d_{so}$$

NERS/BIOE 481 - 2019 5

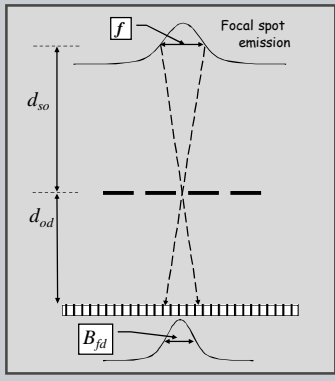
IV.A - Geometric projection (9 charts)

- A) Geometric Projection
 - 1) Transmission geometry
 - 2) Magnification
 - 3) Focal spot blur
 - 4) Object resolution

NERS/BIOE 481 - 2019 3

IV.A.3 - Focal spot blur

Penumbra blur:
The size of the focal spot emission area causes points and edges to be blurred.



Blur for detector dimensions:

$$B_{fd} = f \frac{d_{od}}{d_{so}} = f(M - 1)$$

Blur scaled to object dimensions:

$$B_{fo} = f \frac{(M - 1)}{M} = f \left(1 - \frac{1}{M} \right)$$

NERS/BIOE 481 - 2019 6

IV.A.4 - Object resolution

In general, the detector will further blur the position of incident radiation.

Blur scaled to object dimensions:

$$B_{do} = B_d / M$$

If the focal spot and the detector blur have Gaussian distributions, they convolve to a Gaussian system resolution, scaled to the object, with width, B_o .

$$B_o^2 = B_{do}^2 + B_{fo}^2$$

$$= \left(\frac{B_d}{M}\right)^2 + f^2\left(1 - \frac{1}{M}\right)^2$$

7

IV.A.4 - Object resolution

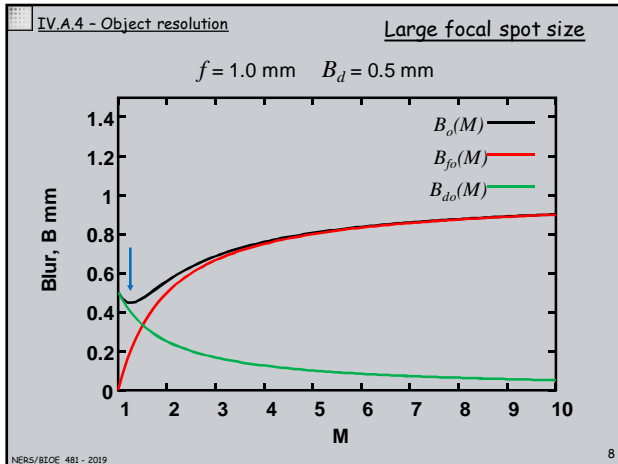
In general, for a given focal spot size and detector blur, there is a magnification that produces minimal resolution in object dimensions. This can be found by setting the derivative of B_o with respect to M equal to 0.

$$B_o^2 = B_{do}^2 + B_{fo}^2 \quad \left| \quad 2B_o \frac{dB_o}{dM} = 2B_{do} \frac{dB_{do}}{dM} + 2B_{fo} \frac{dB_{fo}}{dM} = 0$$

$$B_{do} = \left(\frac{B_d}{M}\right) \quad \left| \quad \frac{dB_{do}}{dM} = \frac{-B_d}{M^2}$$

$$B_{fo} = f\left(1 - \frac{1}{M}\right) \quad \left| \quad \frac{dB_{fo}}{dM} = \frac{f}{M^2}$$

10



IV.A.4 - Object resolution

$$\frac{B_d}{M} \left(\frac{-B_d}{M^2}\right) + f\left(1 - \frac{1}{M}\right) \left(\frac{f}{M^2}\right) = 0$$

Substituting the expressions from the prior page and rearranging yields the simple solution that the best object resolution is obtained when the magnification is equal to 1.0 plus the square of the ratio of the detector blur to the focal spot size.

$$-\frac{B_d^2}{M^3} + f^2\left(1 - \frac{1}{M}\right) = 0$$

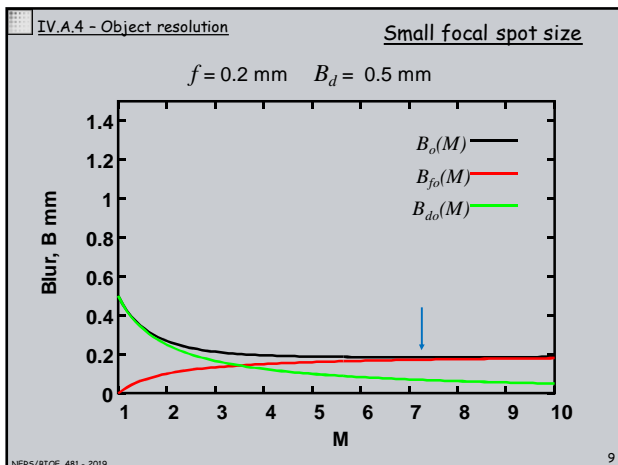
$$-B_d^2 + f^2(M - 1) = 0$$

$$(M - 1) = \left(\frac{B_d}{f}\right)^2$$

$$\Rightarrow M = 1 + \left(\frac{B_d}{f}\right)^2$$

$B_d = 0.5 \text{ mm}, f = 0.2 \text{ mm} \rightarrow M = 7.25$
 $B_d = 0.5 \text{ mm}, f = 1.0 \text{ mm} \rightarrow M = 1.25$

11



IV.A.4 - Example, magnification image Agricultural Imaging

Faxitron X-ray Corp

- MX-20 Digital
- 20 μm focal spot
- 5X magnification

"Ultra-high resolution x-ray imaging is an important tool in seed and plant inspection and analysis."

Sunflower Seed

12

IV.B - Primary Signal (10 charts)

B) Primary Signal - Radiography

- 1) Attenuation
- 2) The projection integral
- 3) Ideal detector
 - a) photon counting
 - b) energy integrating

13

IV.B.2 - projection integral

Radiation traveling through an object along the projection vector p will be subject to attenuation by various material encountered along the path t .

$$\frac{\phi}{\phi_0} = e^{-\mu_1 \Delta t} e^{-\mu_2 \Delta t} e^{-\mu_3 \Delta t} \dots = e^{-\sum_n \mu_n \Delta t} = e^{-\int_0^T \mu(t) dt}$$

16

IV.B.1 - projection nomenclature

To mathematically describe signal and noise, we will consider the signal associated with projection vectors, p , whose directions are defined by detector coordinates, (u, v) , or source angles (θ, ϕ) .

14

IV.B.2 - the Radon transform

- The argument of the exponential factor describing the attenuation through an object path is known as the Radon transform.
- Its form is that of a generalized pathlength integral of a density function.
- The inverse solution to the Radon transform, i.e. $\mu(x, y)$ as a function of $P(r, \theta)$, is used in computed tomography.

$$P(r, \theta) = -\ln\left(\frac{\phi}{\phi_0}\right) = \int_0^r \mu(t) dt$$

In the Radon transform equation above, the attenuation shown as a function of the projection path variable, $\mu(t)$, is more formally written as $\mu(r, \theta)$ or $\mu(x, y)$.

The line integral of $\mu(t)$, $P(r, \theta)$, is referred to as a 'Projection Value'.
The set of all values obtained in one exposure is called a 'Projection View'.

17

IV.B.2 - projection path variable

Radiation traveling along the projection \hat{p} enters the object and will travel a distance T before exiting the object and striking the detector. We will consider a pathlength variable, t , which is 0 at the object entrance and T at exit.

15

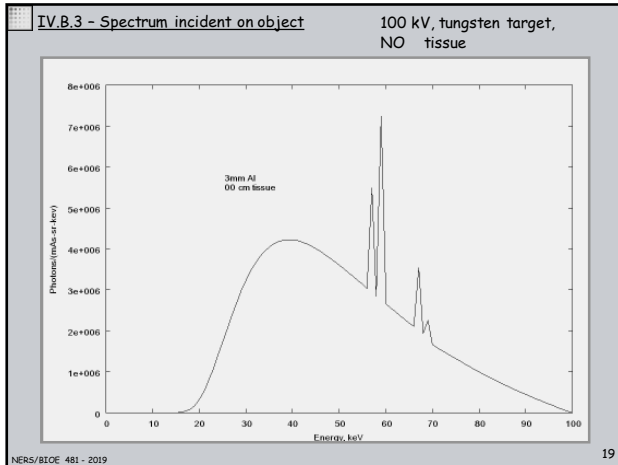
IV.B.3 - Energy dependant incident fluence

- The x-ray fluence on the detector will vary as a function of x-ray energy.

$$\phi^P(E) = \phi_0^P(E) e^{-\int_0^T \mu(t, E) dt}$$

- The energy dependence of the linear attenuation coefficient effects the shape of the differential energy spectrum presented to the detector.

18



IV.B.3 - Ideal image detector - counting type

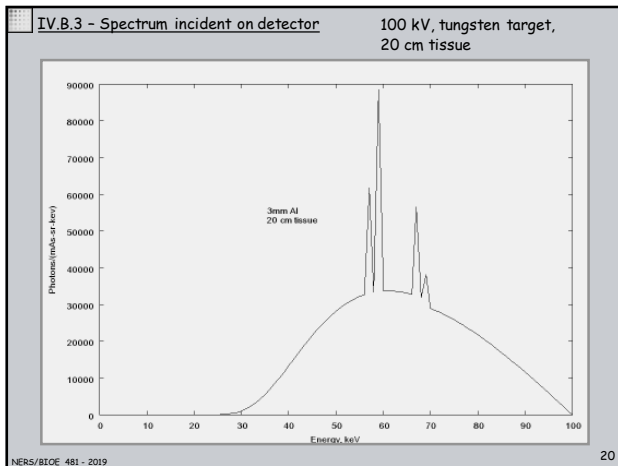
- An ideal **photon counting detector** will accumulate a record of the number of photons incident on the detector surface.
- The detected signal for an ideal photon counting detector, S_c , can be written as:

$$S_c = A_d t \int_0^{E_{\max}} \phi(E) dE$$

Where

- t is the exposure time, sec
- ϕ is the photon fluence rate, photons/mm²/sec,
- A_d is the effective area of a detector element.

22



IV.B.3 - Ideal image detector - energy integrating type

- An ideal **energy integrating detector** will record a signal equal to the total energy of all photons incident on the detector surface.
- The detected signal for an ideal energy integrating detector, S_e , can be written as:

$$S_e = A_d t \int_0^{E_{\max}} E \phi(E) dE$$

Where

- t is the exposure time, sec
- ϕ is the photon fluence rate, photons/mm²/sec,
- A_d is the effective area of a detector element.

The majority of actual radiographic detectors are energy integrating; however, they are not 'ideal'.

23

IV.B.3 - 'ideal' versus actual detectors

- The signals recorded by actual detectors are determined in a complex manner by the energy dependant absorption in the target and background materials and the energy dependant absorption in the detector.
- We consider now signals recorded by 'ideal' detectors. Later we will examine actual detectors

Detector absorption

X-ray photon energy (keV)

Absorption GdCl₂ 0.1 mm

Absorption Cu 0.5 mm

Spectrum 100 kVp 15 cm Al beam

21

IV.C - Radiation Noise & Stats (14 charts)

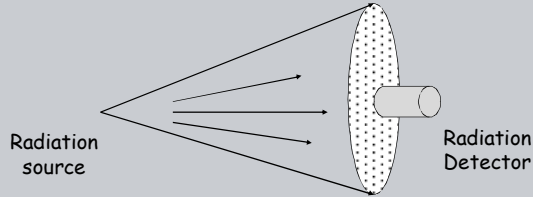
C) **Radiation Detection Noise - Statistical principles**

- 1) Radiation counting & noise
- 2) Poisson/Gaussian distributions
- 3) Propagation of error

24

IV.C.1 - Radiation Counting

A simple radiation detector may be used to make repeated measurements of the number of radiation quanta striking the detector in a specified time period.



IV.C.2 - Poisson distribution of Observed Counts

The "true value" for counted events, m , can be estimated as the average value of many observations;

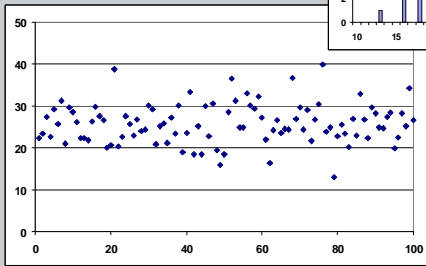
$$m = \sum_{i=1}^n \frac{N_i}{n} = \bar{N}$$

If the detected number of radiation quanta is not correlated from observation to observation, the probability distribution for the observations is given by the Poisson distribution function;

$$P(N) = e^{-m} m^N / N!$$

IV.C.1 - Radiation Counting

100 repeated measure with a mean of 25 and standard deviation of 5 are illustrated.



The number of times that integer values are observed is shown as a bar chart.

IV.C.2 - Variance and Std. Deviation

The width of the Poisson distribution function is described by the variance, σ^2 , which is equal to m ;

$$\sigma^2 = m$$

About 2/3 of the counts will be observed to be in the range from $m-\sigma$ to $m+\sigma$.

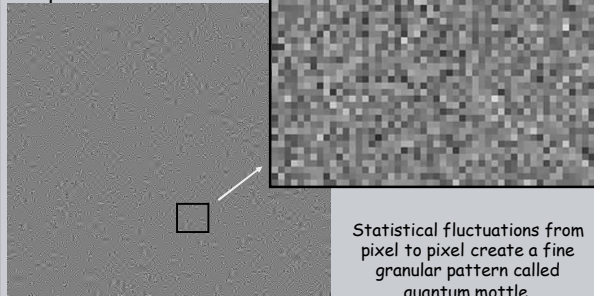
For any single observation, N is about equal to m and therefore;

$$\sigma = \sqrt{N}$$

Relative noise:
$$\frac{\sigma}{N} = \frac{1}{\sqrt{N}}$$

IV.C.1 - Radiation counting, quantum noise (mottle).

Point to point variations about a constant value are distributed similar to repeated measures of one pixel.



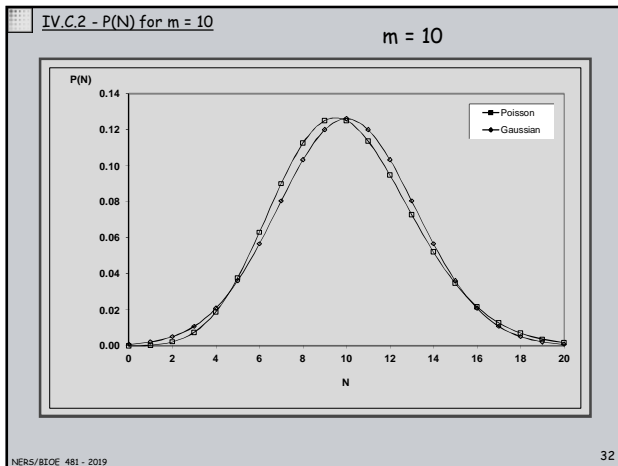
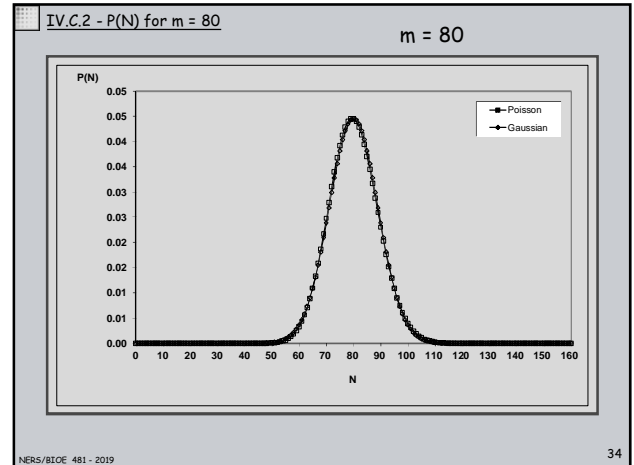
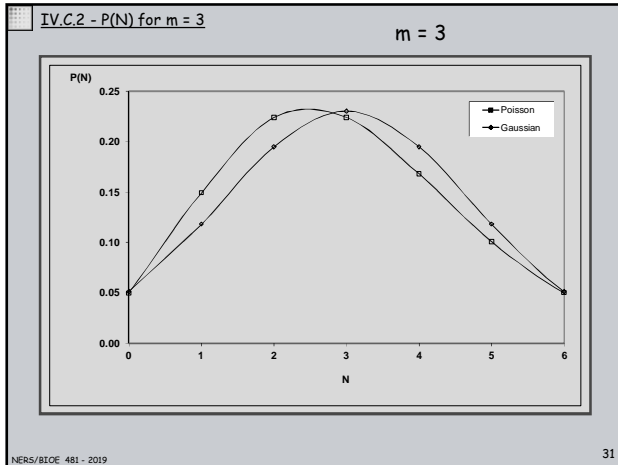
Statistical fluctuations from pixel to pixel create a fine granular pattern called quantum mottle.

IV.C.2 - Gaussian approximation to P(N)

When the mean value, m , is larger than about 20, the Poisson distribution can be approximated by the Gaussian distribution

(also know as the normal distribution);

$$G(N) = \frac{1}{\sigma\sqrt{2\pi}} e^{-\frac{1}{2}\left(\frac{N-m}{\sigma}\right)^2}$$



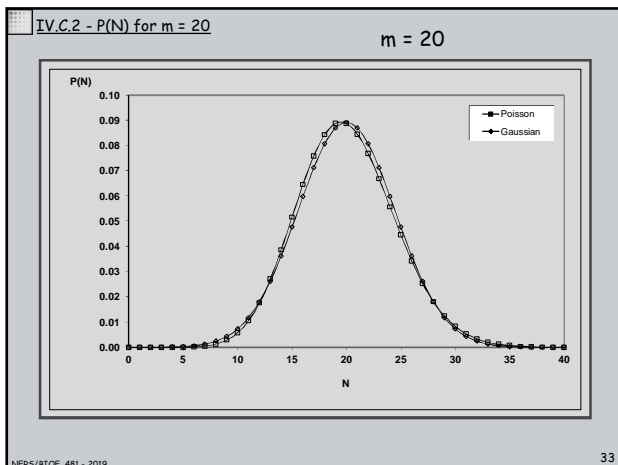
IV.C.3 - Propagation of error.

- Radiation images are typically formed in a sequence of events or operations that lead to the final signal. The signal noise results from any variations associated with individual events or operations.
- If the signal can be expressed as a function, f , which has multiple variables, the noise of the function as a function of the noise of the variables can be deduced from a generalized differential equation.

$$f = f(x, y, \dots)$$

$$\sigma_f^2 = \left(\frac{\partial f}{\partial x}\right)^2 \sigma_x^2 + \left(\frac{\partial f}{\partial y}\right)^2 \sigma_y^2 + \dots$$

NER/S/BIOE 481 - 2019 35



IV.C.3 - Propagation of error, Add/Subtr.

- In the case where the function is the addition or subtraction of terms that depend linearly on x and on y , the noise propagates as the square root of the sum of the weighted squares.

$$f = ax + by$$

$$\sigma_f^2 = a^2 \sigma_x^2 + b^2 \sigma_y^2$$

- This situation arises when a background image is subtracted from an image of an object.

NER/S/BIOE 481 - 2019 36

IV.C.3 - Propagation of error, Mult./Div.

- In the case where the function is the multiplication or division of terms that depend linearly on x and on y, the noise propagates as the square root of the sum of the squared relative noise.

$$f = axy$$

$$\sigma_f^2 = a^2 y^2 \sigma_x^2 + a^2 x^2 \sigma_y^2$$

$$\left(\frac{\sigma_f}{f}\right)^2 = \left(\frac{\sigma_x}{x}\right)^2 + \left(\frac{\sigma_y}{y}\right)^2$$

- This situation arises when we consider the effects of amplifier gain noise and quantum signal noise.

37

IV.D.1 - Monoenergetic signal & noise IDEAL DETECTOR

For an incident x-ray beam for which all x-rays have the same energy, i.e. monoenergetic, the integral expressions for the signal of a counting and of an energy integrating detector reduce to:

$$S_c = (A_d t \phi_E) \quad S_e = E(A_d t \phi_E)$$

The expression in parenthesis, $(A_d t \phi_E)$, is just the number of photons incident on a detector element in the time t . The noise for the counting detector signal is thus just the square root of this expression. For the energy integrating type of device, the noise is weighted by the energy term:

$$\sigma_c = (A_d t \phi_E)^{1/2} \quad \sigma_e = E(A_d t \phi_E)^{1/2}$$

40

IV.C.3 - Propagation of error, Logarithms

- In the case where the function is given by the logarithm of a variable, the function noise is equal to the relative noise of the variable.

$$f = a \ln(x)$$

$$\sigma_f^2 = a^2 \left(\frac{\sigma_x}{x}\right)^2$$

$$\sigma_f = a \frac{\sigma_x}{x}$$

- This situation arises in digital radiography and computed tomography where the image is typically expressed as the logarithm of the recorded signal.

38

IV.D.1 - Monoenergetic signal & noise IDEAL DETECTOR

It is common to relate the amplitude of the signal to that of the noise. The signal to noise ratio, SNR , is high for images with low relative noise.

$$\frac{S_c}{\sigma_c} = (A_d t \phi_E)^{1/2} \quad \frac{S_e}{\sigma_e} = (A_d t \phi_E)^{1/2}$$

For monoenergetic x-rays, the SNR for an ideal energy integrating detector is independent of energy and identical to that of a counting detector. The square of the signal to noise ratio is thus equal to the detector element area time the incident fluence, Φ .

$$\left(\frac{S}{\sigma}\right)^2 = A_d \Phi = N_{eq}$$

For actual detectors recording a spectrum of radiation, the actual SNR^2 is often related to the equivalent number of mono energetic photons that would produce the same SNR with an ideal detector.

Noise Equivalent Quanta (NEQ), N_{eq}

While usually called NEQ , it is typically the Noise Equivalent Fluence, ϕ_{eq} .

41

IV.D - Signal/Noise - ideal detector (6 charts) IDEAL DETECTOR


D) Signal/Noise - ideal detector

- 1) Monoenergetic
- 2) Polyenergetic

39

IV.D.1 - Noise in a medical radiograph

Quantum mottle (noise) in the lower right region of a chest radiograph.



The visibility of anatomic structures is effected by the signal to noise ratio.

42

IV.D.2 - Polyenergetic signal & noise IDEAL DETECTOR

For an ideal photoncounting detector, the signal to noise ratio for a spectrum of radiation is essentially the same as for a monoenergetic beam.

$$\frac{S_c}{\sigma_c} = (A_d t \phi)^{1/2} \quad \phi = \int_0^{E_{\max}} \phi(E) dE$$

For an ideal energy integrating detector, the signal to noise ratio for a spectrum of radiation is more complicated because of the way the energy term influences the signal and the noise integrals.

We saw in the prior section that the signal is given by the first moment integral of the differential fluence spectrum;

$$S_e = A_d t \int_0^{E_{\max}} E \phi(E) dE$$

43

IV.E - Contrast/Noise - ideal detector (14 charts) IDEAL E DETECTOR

E) Contrast/Noise

- 1) Relative contrast and CNR
- 2) CNR for an ideal energy detector
 - Approximate solution
 - Full solution

46

IV.D.2 - Polyenergetic signal & noise IDEAL E DETECTOR

For the noise associated with ideal energy integrating detection of a spectrum of radiation, consider first a discrete spectrum where the fluence incident on the detector at energy E_i is ϕ_i and the signal is;

$$S_e = A_d t \sum_i E_i \phi_i$$

A propagation of error analysis indicates that each discrete component of variance, $E_i^2 (A_d t \phi_i) = E_i^2 (A_d \Phi_i)$, will add to form the total variance. Since A_d is constant, we can express the relationship for signal variance as;

$$\sigma_e^2 = A_d \sum_i E_i^2 \Phi_i$$

Note that for an individual detector element, the above discrete summation is simply equal to the sum of the squared energy deposited in the detector by each photon that strikes the element, $\sum e_i^2$. This is used to estimate signal variance when using Monte Carlo simulations which analyze the interaction of each of a large number of photons.

44

IV.E.1 - Noise in relation to contrast. Images from E. Samei, Duke Univ.

Se Direct Digital Radiographs Chest Phantom

47

IV.D.2 - Polyenergetic signal & noise IDEAL DETECTOR

The corresponding integral expression for the noise of the signal is the second moment integral of the differential energy fluence,

$$\sigma_e^2 = A_d t \int_0^{E_{\max}} E^2 \phi(E) dE$$

And SNR^2 is thus given by;

$$\left(\frac{S_e}{\sigma_e}\right)^2 = A_d t \frac{\left[\int_0^{E_{\max}} E \phi(E) dE\right]^2}{\int_0^{E_{\max}} E^2 \phi(E) dE} = A_d \Phi_{eq}$$

In this case, the noise equivalent quanta (fluence), Φ_{eq} in photons/mm², is given by the ratio of the 1st moment squared to the second moment times the exposure time (Swank, J. Appl. Phys. 1973)

In lecture 7 we will see that the noise power is related to $1/\Phi_{eq}$ with units of mm².

45

IV.E.1 - Signal and Contrast

The visibility of small signal changes depends on the relative signal change in relation to the signal noise

48

IV.E.1 - Relative Contrast

The relative contrast of a target structure is defined as the signal difference between the target and the background divided by the background signal.

$$C = \frac{S_t - S_b}{S_b}$$

$$C_r = \frac{(S_t - S_b)/S_b}{\sigma}$$

49

IV.E.1 - $CNR/(mGy)^{1/2}$

Dose Normalized Contrast to Noise Ratio

$(CNR)^2$

The square of the contrast to noise ratio is proportional to the equivalent number of detected x-ray quanta and thus proportional to mA-s

$(CNR)^2 / Dose$

Since the absorbed dose in the subject is also proportional to mA-s, the ratio of contrast to noise squared to absorbed dose is a logical figure of merit for optimization.

$CNR^2/(mGy)$ or $CNR/(mGy)^{1/2}$

52

IV.E.1 - CNR

Contrast to Noise Ratio

CNR

The ability to detect a small target structure of a particular size is determined by the ratio of the contrast, $(S_t - S_b)$, in relation to the signal noise. **CNR** is equal to the product of the relative contrast and **SNR**.

$$\frac{C}{\sigma} = \frac{S_t - S_b}{\sigma_b} = C_r \frac{S_b}{\sigma_b}$$

50

IV.E.2 - CNR - Approximate solution (Monoenergetic) IDEAL E DETECTOR

- Consider an analysis with the following approximations:
 - homogenous object of uniform thickness, t
 - A δ , thick material perturbation.
 - An ideal energy integrating detector
 - A mono-energetic x-ray beam.
- The relative contrast produced by a small target object results from the difference between the linear attenuation coefficient of the target material, μ_t , and that for the surrounding material, μ_b , which produces the background signal.
- The relationships for the target signal, S_t , and the background signal, S_b , can be written in terms of the fluence incident on the object.
- The relative contrast is thus:

$$C_r = \frac{S_t - S_b}{S_b} = \left(e^{-(\mu_t - \mu_b)\delta_t} - 1 \right) \cong -\Delta\mu\delta_t$$

53

IV.E.1 - The Rose model

Rose showed that small targets are visible if the absolute value of the contrast to noise ratio, $|CNR|$, adjusted for target area is larger than ~4.

S/N - For a target of area A_t , the **SNR** associated with quantum mottle is related to the noise equivalent quanta, Φ_{eq} .

$$\frac{\text{Signal}}{\text{Noise}} = \frac{S}{N} = (A_t \Phi_{eq})^{1/2}$$

C/N - **CNR** is simply the product of the relative contrast and the background **SNR**.

$$\frac{\text{Contrast}}{\text{Noise}} = C_r \frac{S}{N} = C_r (A_t \Phi_{eq})^{1/2}$$

Rose, A
Vision - Human and Electronic
Plenum Press

51

IV.E.2 - CNR - Approximate solution (Monoenergetic) IDEAL E DETECTOR

- The noise variance of the signal in the background can be derived from the background signal equation using the prior results for the propagation of error.
- The noise results from the number of x-ray quanta detected, $A_d \Phi_o e^{-\mu_d t}$, and the energy per quanta, E , is a constant.
- Using the prior expression for the background signal, S_b , the signal to noise ratio may be easily deduced.
- The contrast to noise ratio is then simply obtained by multiplying the **SNR** by the relative contrast derived on the previous page.

$$\sigma_{S_b}^2 = E^2 (A_d \Phi_o e^{-\mu_d t})$$

$$\sigma_{S_b} = E (A_d \Phi_o)^{1/2} e^{-\frac{\mu_d t}{2}}$$

$$\frac{S_b}{\sigma_{S_b}} = \frac{(E (A_d \Phi_o) e^{-\mu_d t})}{\left(E (A_d \Phi_o)^{1/2} e^{-\frac{\mu_d t}{2}} \right)}$$

$$\frac{S_b}{\sigma_{S_b}} = (A_d \Phi_o)^{1/2} e^{-\frac{\mu_d t}{2}}$$

$$\frac{C}{\sigma_{S_b}} = -\Delta\mu\delta_t (A_d \Phi_o)^{1/2} e^{-\frac{\mu_d t}{2}}$$

54

IV.E.2 - CNR - Approximate solution (Monoenergetic) IDEAL E DETECTOR

- The contrast of a small perturbation is intentionally given as the linear attenuation coefficient for the target material, μ_t , minus that for the background material, μ_b .

$$C_r \cong -\Delta\mu\delta_i = -(\mu_t - \mu_b)\delta_i$$

- For the case of a void, $\Delta\mu$ is equal to $-\mu_b$ and C_r will be positive corresponding to an increase in signal at the position of the target.

$$\text{void: } C_r \cong \mu_b\delta_i$$

55

IV.E.2 - CNR - Full solution IDEAL E DETECTOR

- The relative contrast is obtained by considering the ideal energy integrating detector signal for paths thru the detector and thru the target;

$$S_b = A_d \int_0^{kV} E\Phi_o(E)e^{-\int_b \mu(E,s)ds} dE$$

$$S_t = A_d \int_0^{kV} E\Phi_o(E)e^{-\int_t \mu(E,s)ds} dE$$

- In general, these integrals will be evaluated numerically and the relative contrast obtained as the difference divided by the background signal.

58

IV.E.2 - CNR - Approximate solution (Monoenergetic) IDEAL E DETECTOR

Recalling that the attenuation coefficients are strong functions of x-ray energy, $\mu(E)$ can be considered as a variable. CNR for a small void is then of the form, $CNR = kX \exp(-Xt/2)$ where $X = \mu(E)t$.

A rule of thumb based on this approximate solution says that optimal radiographs are obtained with about 10-15 percent transmission thru the object.

56

IV.E.2 - CNR Results - 8 cm breast - W/Sn

Numeric methods (xSpect) were used in 2003 by Dodge (SPIE 2003) to compute $CNR/mGy^{1/2}$ for breast tissue (50-50 BR12) in relation to

- Breast thickness: 4, 6, and 8 cm
- kVp: 10 to 70
- Filter material and thickness

An example of the results is shown at the right where the normalized CNR is plotted in relation to kVp for a tungsten target tube with tin filters.

Flynn, Dodge SPIE 2003

59

IV.E.2 - CNR - Full solution IDEAL E DETECTOR

Slide 45

- In the previous section of this lecture, the SNR for a poly-energetic spectrum was written as;

$$\left(\frac{S_e}{\sigma_e}\right)^2 = A_d t \frac{\left(\int_0^{E_{max}} E\phi(E)dE\right)^2}{\int_0^{E_{max}} E^2\phi(E)dE} = A_d \Phi_{eq}$$

- The CNR for a poly-energetic spectrum is obtained by simply multiplying SNR by the relative contrast.

$$\frac{C}{\sigma_s} = C_r (A_d \Phi_{eq}(kV))^{1/2}$$

- The noise equivalent fluence can be considered as a function of kV (i.e. E_{max}) and written in terms of the incident fluence as;

$$\Phi_{eq}(kV) = \frac{\left(\int_0^{E_{max}} E\Phi_o(E)e^{-\int_b \mu(E,s)ds} dE\right)^2}{\int_0^{E_{max}} E^2\Phi_o(E)e^{-\int_b \mu(E,s)ds} dE}$$

57

IV.E.2 - CNR Results - Moly/Moly vs W/Sn

Mb target with 30 um Mb filter
vs
W target with 50 um Sn filter

T	CNR/mGy ^{1/2}	mA-s/mGy	kVp
4 cm	17.5 16.7	150 105	24.0 / 22
6 cm	9.0 9.5	192 105	24.5 / 26
8 cm	4.6 6.5	230 60	25.0 / 31

Mb-Mb | W-Sn

Flynn, Dodge SPIE 2003

60

IV.F - Advanced Methods (14 charts)

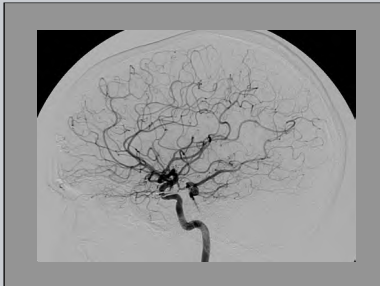
F) Advanced Methods

- 1) Temporal Subtraction
- 2) Dual Energy
- 3) Backscatter
- 4) Phase Contrast

61

IV.F.1 - Temporal Subtraction

The relative contrast between two images can be obtained by subtracting images that are proportional to the log of the detector signal.



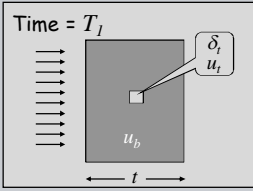
In this Digital Subtraction Angiography (DSA) case, iodinated contrast material has been injected into the right internal carotid artery using a catheter. An image taken just before injection is subtracted from the subsequent images. This patient has a small aneurysm seen at the base of the brain.

64

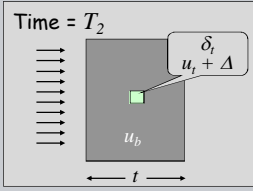
IV.F.1 - Temporal Subtraction (Monoenergetic) IDEAL E DETECTOR

- Consider two radiographs of a fluid target that are obtained at time T_1 and T_2 .
- At T_2 , the target region has increased attenuation due to a soluble contrast agent

Time = T_1



Time = T_2



$$S_b^{T_1} = EA_d \Phi_o e^{-\mu_b t}$$

$$S_i^{T_1} = S_b^{T_1} e^{-(\mu_t - \mu_b) \delta_t}$$

$$S_i^{T_2} = S_b^{T_2} e^{-(\mu_t + \Delta - \mu_b) \delta_t}$$

$$\frac{S_i^{T_1} - S_i^{T_2}}{S_b^{T_1}} = 1 - e^{-\Delta \delta_t} \cong \Delta \delta_t$$

Note: this derivation is based on that in chart 53

62

IV.F.2 - Dual Energy Radiographic Imaging (Monoenergetic)

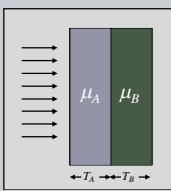
If multiple radiographs of an object are obtained with xray spectra that are significantly different, a linear combination of the images can reveal information about material composition.

$$S^{hi} = S_o^{hi} e^{-(\mu_A^{hi} T_A + \mu_B^{hi} T_B)}$$

$$S^{lo} = S_o^{lo} e^{-(\mu_A^{lo} T_A + \mu_B^{lo} T_B)}$$

$$I_{hi} = \ln(S_o^{hi} / S^{hi}) = \mu_A^{hi} T_A + \mu_B^{hi} T_B$$

$$I_{lo} = \ln(S_o^{lo} / S^{lo}) = \mu_A^{lo} T_A + \mu_B^{lo} T_B$$



The method can be understood by considering an object with two material, A and B, an images I_{hi} and I_{lo} obtained with high and low energy monoenergetic radiation.

65

IV.F.1 - Temporal Subtraction IDEAL E DETECTOR

- For a broad spectrum of radiation, the signals at both times can be evaluated by integrals over the energy dependant fluence and attenuation coefficients.
- It is easier to consider the energy dependant fluence incident on the detector after attenuation by the object.
- The signal difference is then given by an integral of the fluence at the detector times the energy dependant attenuation difference due to the contrast material.

$$S_i^{T_1} = \int EA_d \Phi_o(E) e^{-\mu_b(E)(t - \delta_t)} e^{-\mu_t \delta_t} dE$$

$$= \int EA_d \Phi_{det}^{T_1}(E) dE$$

$$S_i^{T_2} = \int EA_d \Phi_{det}^{T_2}(E) e^{-\Delta(E) \delta_t} dE$$

$$S_i^{T_2} \cong S_i^{T_1} + \int EA_d \Phi_{det}^{T_1}(E) \Delta(E) \delta_t$$

Note: NERS 580 lab 06 has a problem of this type

63

IV.F.2 - Dual Energy Radiographic Imaging (Monoenergetic)

I_B

An image of material B is obtained by multiplying the equation for I_{hi} by w_B and subtracting both sides from the equation for I_{lo} .

$$w_B I_{hi} = \mu_A^{lo} T_A + w_B \mu_B^{hi} T_B$$

$$I_{lo} = \mu_A^{lo} T_A + \mu_B^{lo} T_B$$

$$I_{lo} - w_B I_{hi} = \mu_B^{lo} T_B - w_B \mu_B^{hi} T_B = I_B$$

I_A

An image of material A is obtained by multiplying the equation for I_{hi} by w_A and similarly subtracting both sides from the equation for I_{lo} .

$$w_A I_{hi} = w_A \mu_A^{hi} T_A + \mu_B^{lo} T_B$$

$$I_{lo} = \mu_A^{lo} T_A + \mu_B^{lo} T_B$$

$$I_{lo} - w_A I_{hi} = \mu_A^{lo} T_A - w_A \mu_A^{hi} T_A = I_A$$

66

IV.F.2 - Dual Energy Radiographic Imaging

Low-kVp (a) High-kVp (b)

DE Soft-Tissue (c) DE Bone (d)

Shkumat, Univ. Toronto, 2008

67

IV.F.3 - Backscatter Imaging

Dual Energy Radiograph

Backscatter X-ray

Normal appearance for a briefcase containing two laptop power units with cords and two PDAs.

A detonator cord is wrapped around a laptop power unit and explosives are concealed behind a PDA

American Science and Engr. (AS&E)
<http://www.as-e.com/>

70

IV.F.2 - Dual Energy Radiographic Imaging

Synchronizing the acquisition time of each image to the same phase of the electro-cardiograph (ECG) can reduce motion artifacts from the heart.

Shkumat, Univ Toronto, 2008

68

IV.F.3 - Backscatter Imaging

Dual Energy Radiograph

Backscatter X-ray

Normal appearance for a briefcase containing a large calculator, a laptop power unit, and a PDA

Also contains a Glock handgun and both plastic and liquid explosives

American Science and Engr. (AS&E)
<http://www.as-e.com/>

71

IV.F.3 - Backscatter Imaging

- Backscatter x-ray imaging devices scan the object with a 'pencil' beam of x-rays and measure the radiation backscattered to a large area detector.
- Images using low energy beams emphasize the superficial low Z materials.

American Science and Engr. (AS&E)
<http://www.as-e.com/>

69

IV.F.3 - Backscatter Imaging

American Science and Engr. (AS&E)
<http://www.as-e.com/>

Ammonium Nitrate in trunk

Heroin hidden in body side panel

72

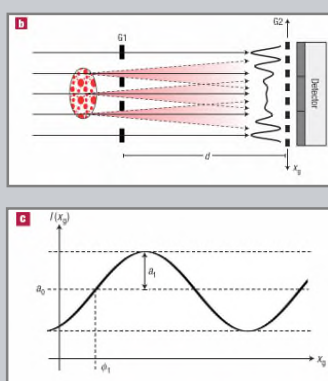
IV.F.4 - Phase Contrast Imaging

- Conventional radiography considers the corpuscular interaction of x-ray absorption to describe attenuation.
- The wave properties of radiation are also effected as radiation travels in a medium. The refractive index, n , of a material describes how EM radiation propagates. $n = c / v$, where
 - c is the speed of light in vacuum and
 - v is the speed of light in the substance.
- For x-rays, n is normally written as a complex number: $n = 1 - \delta + i\beta$, where
 - δ is a small decrement of the real part effecting velocity
 - β is the imaginary part describing absorption.

73

IV.F.4 - Phase Contrast Imaging Pfeiffer 2008 Nature

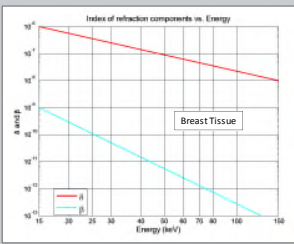
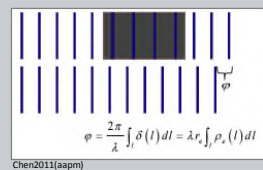
- The $G2$ grating is moved while sequential images are obtained.
- For each pixel, the signal has sinusoidal variation.
- An image can be formed of the amplitude or phase observed for each pixel.



76

IV.F.4 - Phase Contrast Imaging

- While δ is very small, it is substantially larger than β making phase contrast imaging attractive.
- The overall phase shift of the wave is given by a line integral of δ

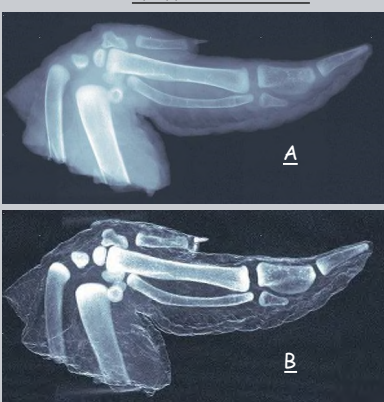
$$\varphi = \frac{2\pi}{\lambda} \int \delta(t) dt = \lambda r \int \rho_e(t) dt$$

74

IV.F.4 - Phase Contrast Imaging Pfeiffer 2008 Nature

A Conventional x-ray transmission image

B 'Dark Field' image proportional to the signal amplitude

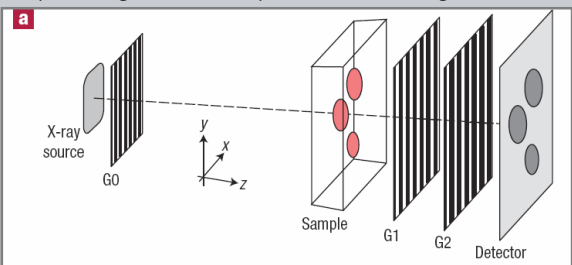


Chicken wing, 40 kV tungsten radiation, 32 mm Si detector

77

IV.F.4 - Phase Contrast Imaging Pfeiffer 2008 Nature

A system consisting of three transmission gratings producing differential phase contrast images.

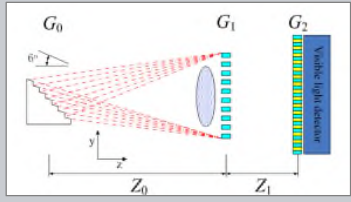
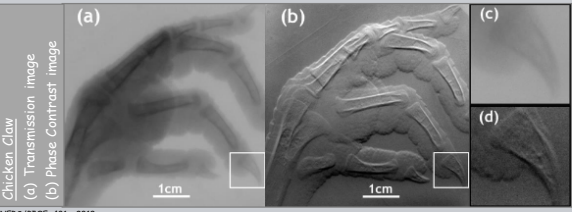


- A set of very narrow sources is created by the $G0$ grating placed in front of an x-ray tube focal spot.
- $G1$ and $G2$ gratings are placed between the object and the detector

75

IV.F.4 - Phase Contrast Imaging Yang Du 2011 Optics Express

- The source grating is non-absorptive.
- A structured scintillator is used as the analyzer grating and detector.

78

IV.F.4 - Phase Contrast Imaging

Zanette 2014 Phys Rev Lett

- A liquid metal target with 8 micron focal spot.
- The source grating is a piece of sandpaper.
- Very high resolution image recording with 9 micron pixels.
- Interference patterns (speckle) are analyzed to deduce phase images.

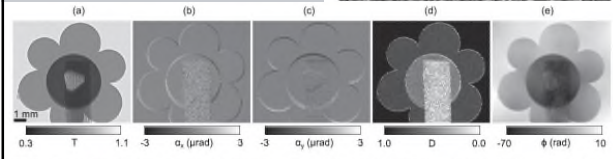
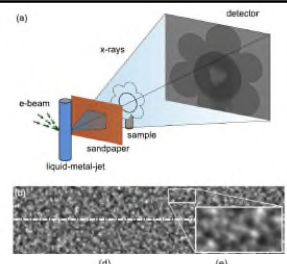


FIG. 3. Speckle-based multimodal images of a plastic flower on a wooden rod. (a) transmission, (b) refraction along x , (c) refraction along y , (d) dark-field, and (e) phase shift.